



# Implementing P-H high speed cornering method on P-PI servo controller with backlash

J. Jahanpour<sup>1</sup> . B. Moetakef Imani<sup>2</sup>

*Mechanical Engineering Department,*

*Ferdowsi University of Mashhad, Mashhad, Iran*

*Corresponding Author E-mail: [imani@ferdowsi.um.ac.ir](mailto:imani@ferdowsi.um.ac.ir)*

## Abstract

In this paper, real-time Pythagorean hodograph (P-H) curve CNC interpolators are used for high speed corner machining. There are large contouring errors around sharp corners when low-bandwidth servo controllers (such as P-PI control) are used. Also backlashes can impose additional errors during tracking a corner. In order to decrease the amount of the cornering errors, an improved interpolation method is proposed. The geometric parameters of the over corner P-H curve and the feed rate along the modified tool path are computed by Pattern Search Algorithm in order to reduce the maximum cornering error. The results of simulation, such as the cornering error and the total cornering time, are compared with previously published methods. It has been observed that the developed over-corner PH approach will substantially reduce the amount of cornering error for P-PI servo controller with backlash.

**Keywords:** P-H curves, CNC interpolators, Cornering error, Backlash

## 1 Introduction

Maintaining the tool path accuracy and the total machining time are among the most important objectives of high speed finishing operations performed on complex parts such as for dies and molds. During machining tool paths with large geometric variations, such as sharp corners, there are either sudden changes of direction on axis movements or sudden stop of motion, which result in large cornering errors.

One method of reducing the tracking error of a sharp corner is to substitute a sharp corner with a smooth curve [1]. Erkorkmaz et al. [2] replaced the line segments of the corner area with two- and three-segment quintic splines. They introduced over-corner and under-corner methods for the P-PI servo controller and the sliding mode controller, respectively.

Pythagorean hodograph (P-H) curves were established by Farouki and Sakkalis [3] in 1990. These curves are a special family of free form curves and a subset of the Bezier representation. The P-H curves are loci with polynomial parameterizations and a special algebraic structure that is uniquely- and well-suited for accurate, efficient and flexible real-time interpolation algorithms. For example, the feed rate can be specified as a function of cumulative arc length or local curvature [4]. In contrast with nearly arc-length parameterization, the arc length of PH curves can be computed precisely by evaluating a polynomial function of the curve parameter [5]. In the following research, the arc-length parametric P-H curve method was proposed

---

<sup>1</sup> - PhD candidate of applied mechanics

<sup>2</sup> - Assistant professor



for the whole corner by Imani and Jahanpour [6], in order to eliminate feed rate fluctuations along the actual tool path. Also, the complexity of the proposed P-H curve interpolation is much lower compared to the interpolation of multi-segment quintic splines.

In this paper, the quadratic velocity interpolation algorithm is proposed for the first deceleration phase of the motion instead of jerk-limited interpolation algorithm. The current work proposes a modified over-corner P-H curve approach for unsymmetrical corners, which are more common in practical applications. The geometric parameters of the over-corner P-H curve and the feed rate along the modified tool path are evaluated using Pattern Search Algorithm [7].

Henceforth, the paper is organized as follows. In Sect. 2, formulation of the P-H quintic is reviewed. In Sect. 3, real-time interpolation using the P-H curve is introduced. The dynamic model of feed drives and the improved over-corner P-H approach are presented in Sects. 4 and 5, respectively. The simulation results are discussed and compared with previous research work in Sect. 6. Finally, Sect. 7 presents the conclusions of the paper.

## 2 Pythagorean hodograph quintic curves

The complex representation for planar P-H curve is given by,  $r(\xi) = x(\xi) + iy(\xi)$ , where  $\xi \in [0,1]$  is a real parameter [5].  $r(\xi)$  is a P-H curve if there exist polynomials  $u(\xi), v(\xi)$  such that its derivative or hodograph,  $r'(\xi) = w(\xi)$  satisfies:

$$x'(\xi) = u^2(\xi) - v^2(\xi), y'(\xi) = 2u(\xi)v(\xi), \sigma(\xi) = u^2(\xi) + v^2(\xi) \quad (1)$$

where  $\sigma(\xi) = \sqrt{x'^2(\xi) + y'^2(\xi)}$  and is the parametric speed of  $r(\xi)$ . The parametric speed of  $r(\xi)$  is the rate of arc length variation with respect to parameter  $\xi$ . Thus, the integration of  $\sigma$  provides the polynomial cumulative arc length function:

$$s(\xi) = \int_0^\xi \sigma(\xi) d\xi \quad (2)$$

For a P-H quintic, the polynomial  $w(\xi) = u(\xi) + iv(\xi)$  must be quadratic. Expressing in Bernstein form, the hodograph is:

$$r'(\xi) = [w_0(1-\xi)^2 + w_1 2(1-\xi)\xi + w_2 \xi^2]^2 \quad (3)$$

Considering the interpolation conditions, the P-H quintic curves which interpolate the given end-points and end-derivatives are obtained by the following coefficients, further details will be found in [6]:

$$w_0 = \pm\sqrt{d_0}, w_2 = \pm\sqrt{d_1} \quad (4)$$

$$w_1 = \frac{-3(w_0 + w_2) \pm \sqrt{120(r_1 - r_0) - 15w_0^2 - 15w_2^2 + 10w_0w_2}}{4} \quad (5)$$

where  $r_0, r_1$  are end-points and  $d_0, d_1$  are corresponding end-derivatives. Taking into account the signs of  $w_0, w_1$  and  $w_2$ , there are four independent P-H quintic interpolants. Moon et al. [5] have recommended the absolute rotation index to select the acceptable shape.



### 3 Real-time interpolation by P-H quintic curves

Real-time interpolation by P-H quintic curves was proposed by Farouki and Sagar [8] in 1995. They firstly presented formulations and analyses where the feed rate on the P-H curve is specified as a constant, linear, or quadratic function of the arc length.

For constant feed rate, the arc length value is:

$$s(\xi_k) = k\Delta s_0 \quad (6)$$

where  $\Delta s_0 = V_c \Delta t$  is the arc length in iteration  $k$ ,  $\Delta t$  is the sampling period and  $V_c$  is the constant feed rate. The desired sequence of parameter values  $\xi_1, \xi_2, \dots, \xi_N$  is computed by equation (6). This equation has a unique real root  $\xi_k$ , which can be determined using Newton-Raphson method as follows [8]:

$$\xi_k^{(r)} = \xi_k^{(r-1)} - \frac{s(\xi_k^{(r-1)}) - k\Delta s_0}{\sigma(\xi_k^{(r-1)})}, \quad r = 1, 2, \dots \quad (7)$$

The feed rate variation in the case of a quadratic function of arc length is:

$$V(s) = V_0(1-s/S)^2 + 2V_1(1-s/S)(s/S) + V_2(s/S)^2 \quad (8)$$

where  $S$  is the length of curve,  $s$  is the cumulative arc length, and  $V_0$  and  $V_2$  are the feed rates at the first and end points of the P-H curve, respectively. The feed rate is defined by:  $V(s) = ds/dt$  and can be rewritten as:  $dt = ds/V(s)$

The integration from this equation yields:

$$\int_{s_{k-1}}^{s_k} ds/V(s) = \Delta t \quad (9)$$

where  $s_{k-1} = s(\xi_{k-1})$  and  $s_k = s(\xi_k)$  are cumulative arc length for  $\xi_{k-1}$  and  $\xi_k$ , respectively. The analytical reduction of equation (9) is computed by substitution of  $V(s)$ . The solution of this integral depends on the sign of the  $E = V_1^2 - V_0V_2$ . [8]

Considering  $E > 0$  and defining  $V_*$  and  $V'$ , as follows:

$$V_* = \sqrt{V_1^2 - V_0V_2}, \quad V'(s) = (V_1 - V_0)(1-s/S) + (V_2 - V_1)(s/S) \quad (10)$$

The integration of equation (9) results in:

$$s(\xi_k) = \frac{V_*\phi(\xi_{k-1}) - V_1 + V_0}{V_2 - 2V_1 + V_0} S, \quad (11)$$

$$\phi(\xi_{k-1}) = \frac{V'(s(\xi_{k-1})) - V_* \tanh(V_* \Delta t / S)}{V_* - V'(s(\xi_{k-1})) \tanh(V_* \Delta t / S)}$$

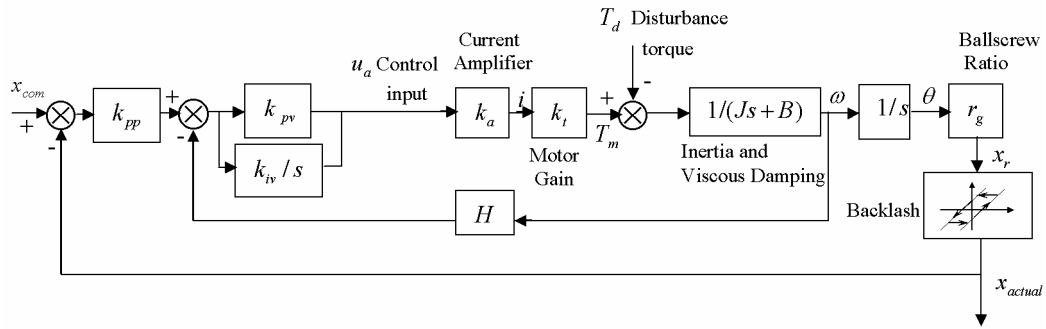


Figure 1: Block diagram of the P-PI servo controller with backlash

Equation (11) also has unique real root, which can be accurately determined using the Newton-Raphson iterations.

For the quadratic velocity interpolation,  $S_{\min.all}$  the minimum allowable curve length of the acceleration/deceleration phase of motion depends on the physical limits of the drive system. [9]. A Matlab code is written to keep the maximum deceleration and jerk within allowable physical limits. Based on given feed rates at the first and end point of deceleration phase, an iterative algorithm starts with an initial approximation for curve length, which is obtained from the jerk-limited algorithm [10]. In the following step, the maximum deceleration and jerk are computed and compared with the physical limits. In the final step, the value of the curve length is increased by small amount of  $\Delta s$ . This procedure is continued until the limitations of deceleration and jerk, are satisfied.

#### 4 Dynamic model of the feed drive

The linear dynamic model of a P-PI servo controller defined for classical feed drives is shown in Figure1. This controller is a commonly used structure in CNC drive systems [2, 11].  $u_a$  [v],  $k_a$  [A/v],  $i$  [A] and  $k_t$  [N.m/A] are in sequence the control signal, the current amplifier, the motor current, and the motor gain, respectively. The other parameters are defined in Table 1. The feedback control law in Laplace domain is written as follows:

$$u_a(s) = [(x_{com} - x_{act})k_{pp} - H\omega(s)](k_{pv} + \frac{k_{iv}}{s}) \quad (12)$$

where  $H$  [v.s/rad] is the velocity feedback gain and the angular velocity and actual rigid position are expressed by:

$$\omega(s) = \frac{k_t k_a}{Js + B} u_a(s), \quad x_r(s) = \frac{r_g}{s} \omega(s) = \frac{r_g}{s} \cdot \frac{k_t k_a}{Js + B} u_a(s) \quad (13)$$

In the above relation  $r_g$  [mm/rad] is the transmission ratio.  $x_{act}$ , the actual position is evaluated regarding backlash effects. The backlash model, which has been adopted in this article, will be found in [11]. The feed-drive and the controller parameters are chosen according to [11]. These parameters are summarized in Table1.



## 5 The developed over-corner P-H curve approach

The developed over-corner P-H approach is based on the following idea. One P-H curve is constructed over the corner region. The position commands are then generated using the newly constructed P-H curve. Consequently, in spite of backlash of ball screw drives, which is 7  $\mu\text{m}$ , the actual tool path gets closer to the linear segments of the corner and maintains the overall cornering error within a certain limit. Also with this approach, the tool turns around the sharp corner without stopping. The geometry of modified tool path for over-corner P-H approach is introduced in Figure 2.  $c_1$  and  $c_2$  are the distance of start- and end-point of P-H curve from the corner tip,  $P_{cor}$ . The start- and end-point positions of P-H curve are:

$$r_0 = (L - c_1) \sin \alpha + (L - c_1) \cos \alpha \ i \quad , \quad r_1 = (L \sin \alpha + c_2 \sin \beta) + (L \cos \alpha - c_2 \cos \beta) \ i \quad (14)$$

where  $L$  is the length of the corner edge, and  $\alpha$  and  $\beta$  are the angle of linear segments of the corner with vertical axis. The start and end derivatives are given by:

$$d_0 = 1 + \tan \beta_1 \ i \quad , \quad d_1 = 1 - \tan \beta_2 \ i \quad (15)$$

where  $\beta_1$  and  $\beta_2$  are:

$$\beta_1 = \pi/2 - \alpha - \gamma_1 \quad , \quad \beta_2 = \pi/2 - \beta + \gamma_2 \quad (16)$$

In the above relations,  $\gamma_1$  and  $\gamma_2$  are the correction angles for start- and end-point of the P-H curve, respectively. The corrected end-derivatives are:

$$d'_0 = b_1 [1 + \tan(\pi/2 - \alpha - \gamma_1) \ i] \quad , \quad d'_1 = b_2 [1 - \tan(\pi/2 - \beta + \gamma_2) \ i] \quad (17)$$

where  $b_1$  and  $b_2$  are end-derivative magnitude coefficients.[6]

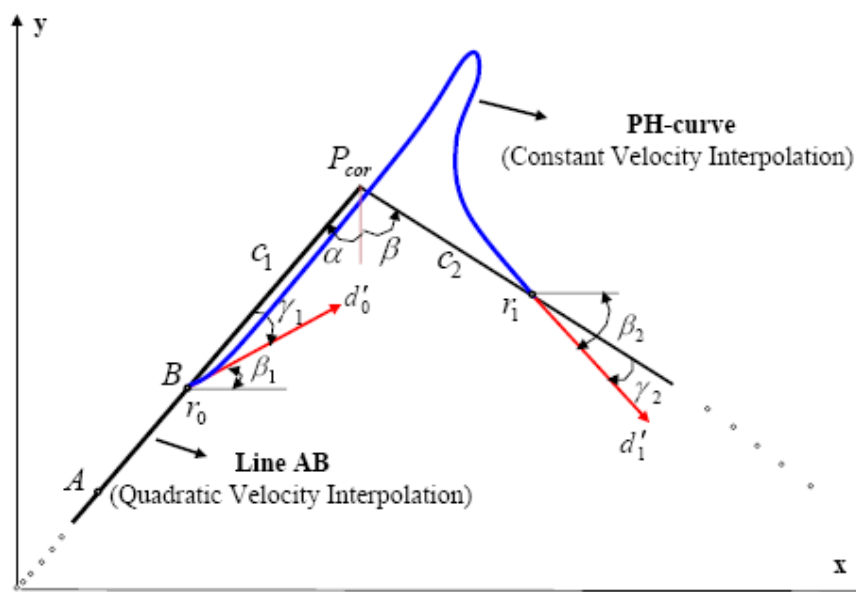


Figure 2: Geometry of an unsymmetrical corner and over-corner P-H tool path



The minimization of the cornering error is implemented based on Matlab's Pattern Search Algorithm [7], as follows: optimization variables are  $\gamma_1, b_1, \gamma_2, b_2, c_1, c_2$  and  $V_c$ . In stage 1: the quadratic velocity interpolation for line AB is implemented. In stage 2: the over-corner P-H curve and real-time interpolation are computed. In the following stage, using the input variables, the generated commands are input to the P-PI servo controller. In this way actual tool path positions are obtained by time iteration of the whole algorithm. Finally the corner error profile between actual and reference tool path is evaluated. The objective function which is minimized using Pattern Search Algorithm is: The maximum cornering error. Further details can be found in [12].

## 6 Simulations

The original tool path consists of two 50 -mm linear segments. A constant feed rate of 100 mm/s is used for traveling along linear segments. The maximum jerk of 50,000 mm/s<sup>3</sup> and maximum acceleration of 2,000 mm/s<sup>2</sup> are used. In all cases,  $\Delta t$  is equal to 1ms and  $\Delta s$  is equal to 0.005 mm. The start point, lower bounds, and upper bounds of the parameters used in Pattern Search Algorithm (P.S.A) are given in Table 2. Also, the selected options for P.S.A are adapted to Matlab-P.S.A defaults. Thus, are not mentioned. The geometric parameters of the over-corner P-H curve and the feed rate are presented in Table 3.

The Simulation results for the case of  $\alpha=90^\circ, \beta=0^\circ$  are shown in Figure 3 and Figure 4. In Figure 3 (a) it can be observed that the P-PI controller is not able to follow the sharp corner correctly and there is a large cornering error. The maximum cornering error is about 306.1  $\mu\text{m}$ , which is shown in Figure 3 (b). The modified tool path with the P-H curve is shown in Figure 4 (a). The actual tool path is also depicted. The commands generated using the quadratic velocity interpolation, in deceleration phase of the motion, is shown with a larger scale in Detail 1 of Figure 4 (a). As can be seen, the arc length is decreasing at each sampling period and reaching to the constant arc length, which is traveled along over P-H curve, shown in Detail 2 of Figure 4 (a). The deviation error of the actual tool path from the original tool path is shown in Figure 4 (b). It can be observed that the maximum cornering error is equal to 3.19  $\mu\text{m}$ . The feed rate profile is shown in Figure 5 and denoted by the feed rate interpolation phases. The computed minimum curve length in deceleration phase of the motion is equal to 6.15 mm. As can be seen in Figure 6, this minimum curve length satisfies the jerk constraint, which is assumed to be 50,000 mm/s<sup>3</sup>. Although the total corner machining time is increased by small amount of 13.42% with respect to the original tool path, the amount of maximum cornering error is decreased and reached to the allowable tight tolerance limit, which is assumed to be 5  $\mu\text{m}$ . The results of Pattern Search Algorithm for this case are shown in Figure 7. As can be seen, the maximum cornering error using the above initial point is equal to 41.5  $\mu\text{m}$ , which converges and reduces to 3.19  $\mu\text{m}$  after 70 iterations. The total number of function evaluations is equal to 223.

Simulation results for the symmetrical corner with angles  $\alpha=30^\circ, \beta=30^\circ$ , are shown in Figs.8 and 9. There is a large cornering error equal to 318.4  $\mu\text{m}$  which is shown in Figure 8 (b). The modified tool path with the P-H curve is shown in Figure 9 (a). The actual tool path is also depicted. The deviation error of the actual tool path from the original tool path is shown in Figure 9 (b). It can be observed that the maximum cornering error is 3.16  $\mu\text{m}$ . The simulation results of the proposed method for this case shows that the amount of cornering error is improved by about 600%



compared with the results reported in [6], while the total machining time is not increased.

Table 1: Feed drive and controller parameters

| <b>Feed drive parameters</b>                      | <b>X-axis</b> | <b>Y-axis</b> |
|---|---------------|---------------|
| Current amplifier gain, $k_a$ (A/V)               | 6.4898        | 7.5768        |
| Motor gain, $k_t$ (Nm/A)                          | 0.4769        | 0.4769        |
| Total reflected inertia, $J$ (kg m <sup>2</sup> ) | 0.007773      | 0.009811      |
| Viscous damping, $B$ (kg m <sup>2</sup> /s)       | 0.019811      | 0.028438      |
| Transmission gain, $r_g$ (mm/rad)                 | 1.5915        | 1.5915        |
| Backlash of ball-screw ( $\mu$ m)                 | 7             | 7             |
| <b>PI Control parameters for velocity loop:</b>   |               |               |
| Velocity feedback gain, $H$ (Vs/rad)              | 1             | 1             |
| Proportional gain, $k_{pv}$ (V/V)                 | 1             | 1             |
| Integral gain, $k_{iv}$ (V/V)                     | 0.5           | 0.5           |
| <b>P Control parameter for position loop:</b>     |               |               |
| Proportional gain, $k_{pp}$ (V/mm):               | 20.1          | 20.1          |

Table 2: Start point, lower and upper bounds of the parameters in Pattern Search Algorithm

|                                   |              | $b_1$ | $b_2$ | $c_1$ | $c_2$ | $\gamma_1$ | $\gamma_2$ | $V_c$ |
|-----------------------------------|--------------|-------|-------|-------|-------|------------|------------|-------|
|                                   | Lower bounds | 2     | 1.2   | 0.12  | 0.12  | -3         | 1          | 3     |
| $\alpha=90^\circ, \beta=0^\circ$  | Upper bounds | 2.5   | 1.5   | 0.2   | 0.2   | 0          | 2          | 4     |
|                                   | Start point  | 2.1   | 1.35  | 0.13  | 0.13  | -1.6       | 1.6        | 3.6   |
|                                   |              |       |       |       |       |            |            |       |
|                                   | Lower bounds | 0.8   | 0.5   | 0.12  | 0.12  | -2         | -4         | 3     |
| $\alpha=30^\circ, \beta=30^\circ$ | Upper bounds | 1     | 0.9   | 0.2   | 0.15  | 0          | -1         | 4     |
|                                   | Start point  | 0.9   | 0.6   | 0.13  | 0.14  | -0.5       | -2         | 3.5   |

Table 3: Geometric parameters of the over-corner P-H curves and the feed rate, computed by Pattern Search Algorithm

| <b>P-H parameters</b> | $\alpha=90^\circ, \beta=0^\circ$ | $\alpha=30^\circ, \beta=30^\circ$ |
|-----------------------|----------------------------------|-----------------------------------|
| $b_1$                 | 2.4146                           | 0.96                              |
| $b_2$                 | 1.4445                           | 0.76                              |
| $\gamma_1(^{\circ})$  | -1.5098                          | -1.002                            |
| $\gamma_2(^{\circ})$  | 1.8                              | -3.1                              |
| $c_1$ (mm)            | 0.138                            | 0.120                             |
| $c_2$ (mm)            | 0.14                             | 0.131                             |
| $V_c$ (mm/s)          | 3.82                             | 3.65                              |

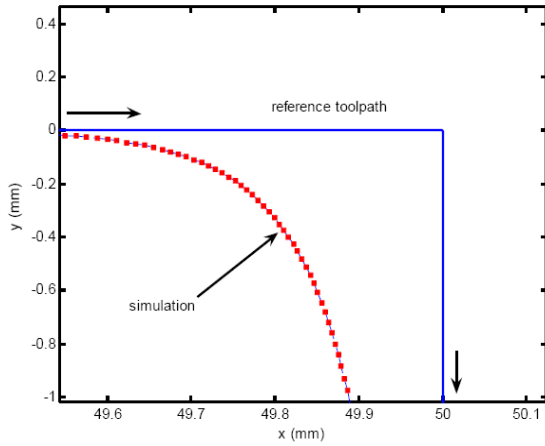


Figure 3 (a): Cornering performance

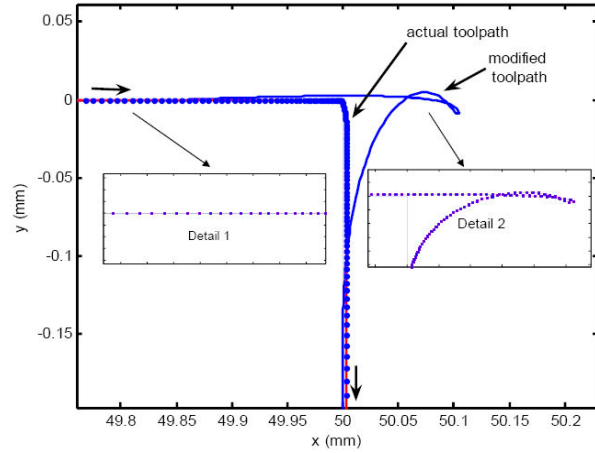


Figure 4 (a): Cornering performance

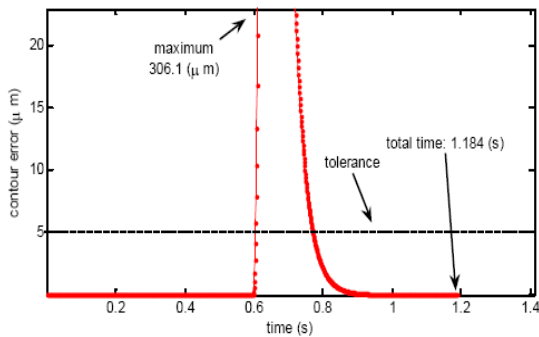


Figure 3 (b): Cornering error profile

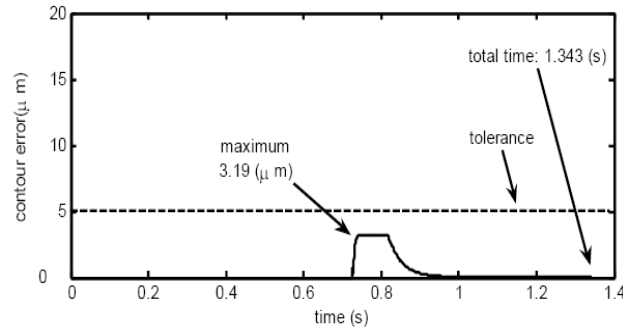


Figure 4 (b): Cornering error profile

Figure 3: Original tool path performance for  $\alpha=90^\circ$ ,  $\beta=0^\circ$  with the P-PI servo controller

Figure 4: Modified tool path performance for  $\alpha=90^\circ$ ,  $\beta=0^\circ$  over-corner P-H curve with the P-PI servo controller

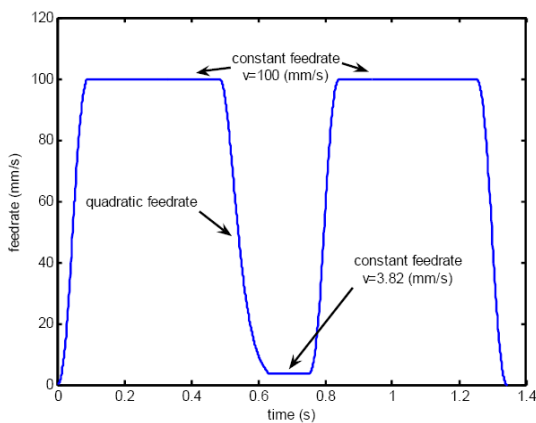


Figure 5: Modified feed rate profile for the corner:  $\alpha=90^\circ$ ,  $\beta=0^\circ$

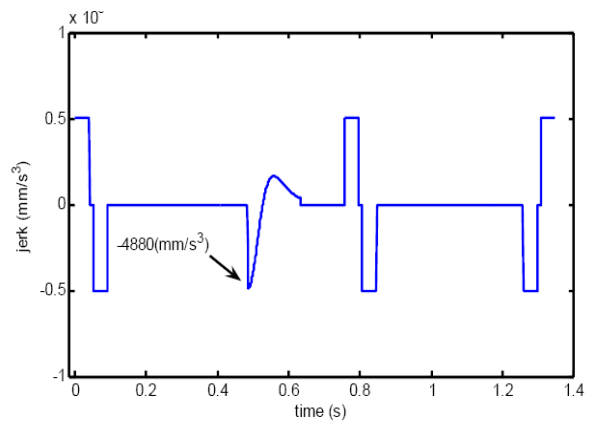


Figure 6: Modified jerk profile for the corner:  $\alpha=90^\circ$ ,  $\beta=0^\circ$



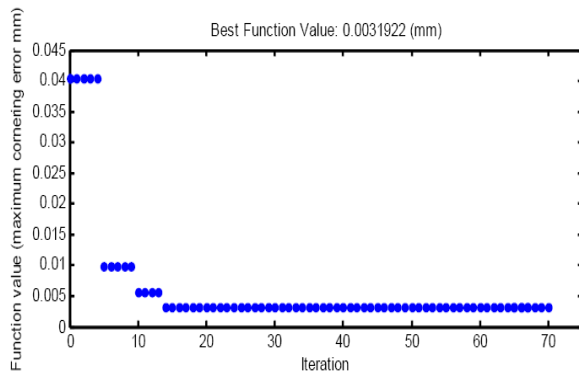


Figure 7 (a): Best function value

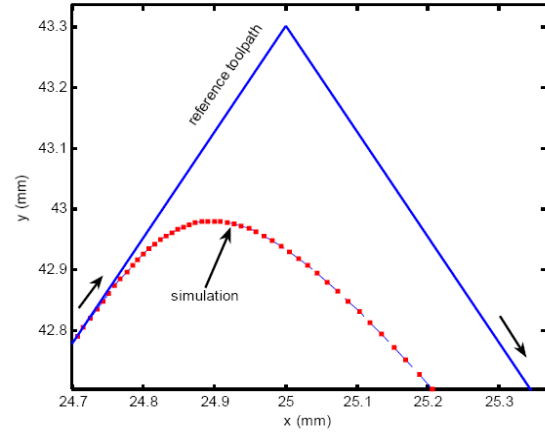


Figure 8 (a): Cornering performance

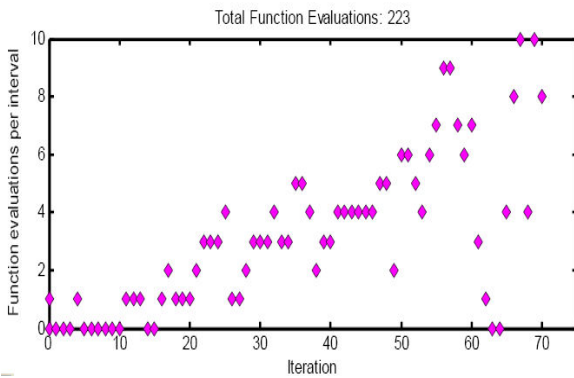


Figure 7 (b): Number of function evaluations per interval

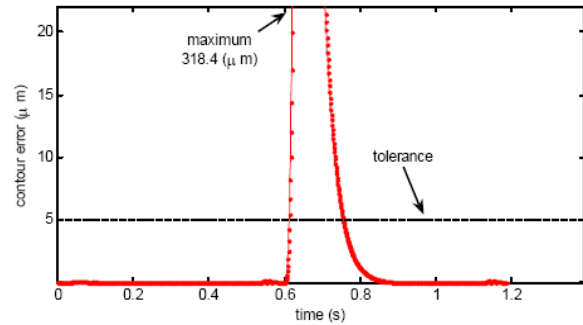


Figure 8 (b): Cornering error profile

Figure 8: Original tool path performance for  $\alpha=30^\circ$ ,  $\beta=30^\circ$  with the P-PI servo controller

Figure 7: Pattern Search Algorithm results for  $\alpha=90^\circ$ ,  $\beta=0^\circ$

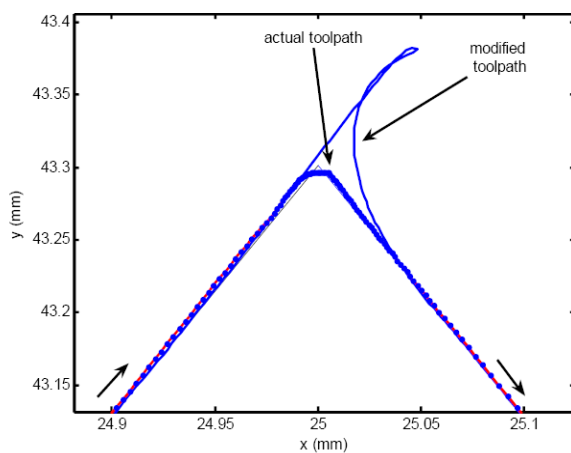


Figure 9 (a): Cornering performance

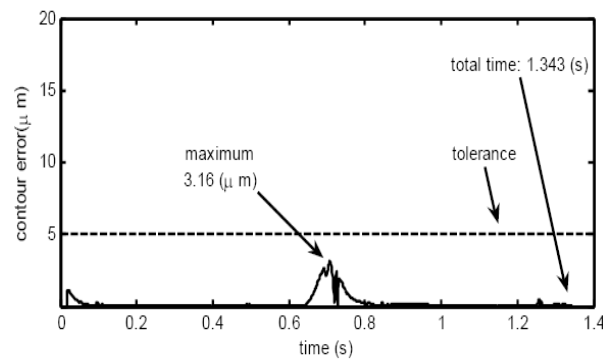


Figure 9 (b): Cornering error profile

Figure 9: Modified tool path performance for  $\alpha=30^\circ$ ,  $\beta=30^\circ$  over-corner P-H curve with the P-PI servo controller



## 7 Conclusions

The method presented for corner machining is based on real-time P-H curve CNC interpolators' theory. Compared with the previously proposed method, which used the jerk-limited algorithm for the first deceleration phase of the motion, the newly developed over-corner P-H curve approach proposes a combination of the quadratic velocity interpolation in deceleration phase of the motion and the constant velocity interpolation on the over corner P-H curve. As a result, the maximum cornering error will be reduce significantly. The geometric parameters of the over corner P-H curve, such as end-points, end-derivatives and correction angles along with feed rate for the over corner P-H curve, are computed by Pattern Search Algorithm according to the corner angle and physical constraints. The simulation results for symmetrical and unsymmetrical corners for P-PI servo controller with backlash confirm that the modified over-corner P-H approach is capable of decreasing the corner error and maintaining the tracking accuracy within a certain limit.

## References

- [1] M.K. Jouaneh and Z. Wang and Dornfeld D.A " Trajectory planning for coordinated motion of a robot and a positioning table. Part 1.Path specification ", IEEE Trans on Robotics and Automation, Vol.6, n 6 (1990), pp 735-745.
- [2] K. Erkorkmaz and C.H. Yeung and Y.Altintas " Virtual CNC System. Part II. High speed contouring application ", Int J of Machine Tools and Manufacture, Vol.46, n10 (2006), pp 1124-1138.
- [3] R.T. Farouki and T. Sakkalis " Pythagorean Hodographs", IBM J of Research and Development, Vol.34, n 5 (1990), pp 736-752.
- [4] S.D. Timar and R.T. Farouki and T.S. Smith and C.L. Boyadjieff " Algorithms for time-optimal control of CNC machines along curved tool paths" , Robotics and computer-integrated manuf, Vol.21(2005), pp 37-53.
- [5] H.P. Moon and R.T. Farouki and H.I. Choi " Construction and shape analysis of PH quintic Hermite interpolants", Comput Aided Geom Des, Vol.18(2001), pp 93-115.
- [6] B.M. Imani and J. Jahanpour " High speed contouring enhanced with P-H curves", Int J Adv Manuf Technol, (2007) DOI 10.1007/s00170-007-1006-z.
- [7] R.M. Lewis and V. Torczon " Pattern Search Algorithms for Bound Constrained Minimization", SIAM Journal on Optimization, Vol.9(4) (1999), pp 1082 – 1099.
- [8] R.T. Farouki and Shah. Sagar " Real-time CNC interpolators for Pythagorean-hodograph curves", Comput Aided Geom Des, Vol.13(1995), pp 583-600.
- [9] R.T. Farouki and Y.F. Tsai and C.S. Wilson " Physical constraints on feed rates and feed accelerations along curved tool paths", Comput Aided Geom Des, Vol.17 (2000), pp 337-359.
- [10] K. Erkorkmaz andY. Altintas " High speed CNC system design .Part I: Jerk limited trajectory generation and quintic spline interpolation", Int J of Machine Tools and Manufacture, Vol.41 (2001), pp 1323-1345.
- [11] C.H. Yeung and Y. Altintas and K. Erkorkmaz " Virtual CNC System. Part I. System architecture", Int J of Machine Tools and Manufacture, Vol.46, n10 (2006), pp 1107-1123.
- [12] J. Jahanpour and B.M. Imani " Real-time P-H curve CNC interpolators for High speed cornering ", Int J Adv Manuf Technol, (2007) DOI 10.1007/s00170-007-1217-3.